PROCEEDINGS OF SPIE

SPIE—The International Society for Optical Engineering

Optomechanics 2003

Alson E. Hatheway
Chair/Editor

7–8 August 2003
San Diego, California, USA

SPIE PROCEEDINGS SERIES

Volume 5176

PROCEEDINGS OF SPIE
SPIE—The International Society for Optical Engineering

Optomechanics 2003

Alson E. Hatheway
Chair/Editor

7–8 August 2003
San Diego, California, USA

Sponsored and Published by
SPIE—The International Society for Optical Engineering

SPIE
P
PROCEEDINGS SERIES

Volume 5176

The papers published in this volume compose the proceedings of the technical conference cited on the cover and title page. Papers were selected by the conference program committee to be presented in oral or poster format, and were subject to review by the editors and program committee. They are published herein as submitted, in the interest of timely dissemination.

Please use the following format to cite material from this book:

Author(s), "Title of Paper," in Proceedings of SPIE Vol. 5176 *Optomechanics 2003*, edited by Alson E. Hatheway (SPIE, Bellingham, WA, 2003) page numbers.

ISSN 0277-786X
ISBN 0-8194-5049-9

Published by
SPIE—The International Society for Optical Engineering
P.O. Box 10, Bellingham, Washington 98227-0010 USA
Telephone 1 360/676-3290 (Pacific Time) · Fax 1 360/647-1445

Printed in the United States of America.

Conference Committee

Symposium Chair

Glenn D. Boreman, CREOL, University of Central Florida (USA)

Conference Chair

Alson E. Hatheway, Alson E. Hatheway, Inc. (USA)

Program Committee

Anees Ahmad, Raytheon Company (USA)
Patrick A. Bournes, Iolon, Inc. (USA)
John M. Casstevens, Dallas Optical Systems, Inc. (USA)
Robert G. Chave, RCAP, Inc. (USA)
Eri J. Cohen, Jet Propulsion Laboratory (USA)
John G. Daly, Vector Engineering, Inc. (USA)
Keith B. Doyle, Sigmadyne, Inc. (USA)
Tony Hull, Jet Propulsion Laboratory (USA)
José M. Sasián, Optical Sciences Center, University of Arizona (USA)
Ann F. Shipley, University of Colorado, Boulder (USA)
Deming Shu, Argonne National Laboratory (USA)
Daniel Vukobratovich, Raytheon Company (USA)
Paul R. Yoder, Jr., Consultant in Optical Engineering (USA)
Carl H. Zweben, Composites Consultant (USA)

Contents

Transferring FEA results to optics codes with Zernikes: a review of techniques

Patrick A. Coronato* and Richard C. Juergens
Raytheon Missile Systems, 1151 E. Hermans Road, MS 840/4, Tucson, AZ, USA 86706

ABSTRACT

The detailed displacement data provided by finite element analysis (FEA) tools must be translated into forms acceptable by most optical ray tracing tools (CODE V specifically). A useful medium for transferring FEA data is the Zernike circular polynomials that many optical ray tracing tools will readily accept as input. However, the translation process is nontrivial, and two specific difficulties are explored in this paper. The first issue involves a coordinate space transformation that is required because the optically relevant coordinate system is not the same as the Cartesian coordinate system typically used in the finite element model. Several algorithms are described to perform this transformation and their pros and cons enumerated. Specifically, comparisons are made between sag based and surface normal (wavefront) based coordinate systems, and it is found that by using the sag equation of the original surface, the accuracy of the data translation can be improved. The second issue discussed is the accuracy of the polynomial fitting process. The loss of orthogonality stemming from undersampling, nonuniform mesh density, and annular surfaces are discussed with potential work-arounds.

Keywords: opto-mechanical analysis, Zernike polynomials, orthogonality, optical deformations, data fitting, FEA

1. INTRODUCTION

In the optical-mechanical analysis domain, we have found that it is useful to use Zernike polynomials to model the optical surface deformations computed by finite element analysis (FEA). This in itself is not such a novel idea[1,2] and two commercially available computer programs currently exist to perform this task[3,4].

However, our use of these programs and subsequent investigations uncovered numerous subtle approximations and error sources that should be understood when trying to implement Zernike fitting of FEA data. This paper describes several techniques of transforming FEA data into optically relevant Zernike polynomials, describes the pros and cons of each, and hopes to shed light on the nuances of implementation of, what we consider, a powerful process enhancement.

2. MOTIVATION

There are several efficiencies to be gained by using Zernike polynomials to represent FEA deformations of optical surfaces. Two of the most compelling are data compaction and transportability, and the transformation of an abstruse matrix of data into useful opto-mechanical information.

The data generated by FEA is voluminous. With a few keystrokes and a couple of seconds, an optical surface can be meshed with thousands of gridpoints (or nodes), each of which can have between three and five distinct deformations for each loading condition. By using Zernike polynomials, this massive amount of FEA nodal deformation information can be efficiently compressed into a relatively small (<100) list of numbers representing scaling coefficients of those polynomials. Most optical analysis programs currently support the incorporation of optical surface deformations as lists of Zernike polynomial scaling coefficients, so the FEA data becomes transportable between multiple analysis programs without having to write and maintain an FEA translator into each different optical analysis program.

* E-mail: Patrick_A_Coronato@raytheon.com, Telephone: 520-794-0639

Besides data transfer efficiencies, there are also advantages gained by transforming Cartesian or cylindrical mechanical deformations into more tractable optical concepts. Because the Zernike polynomials resemble common optical aberrations, decomposing FEA deformations into a set of Zernike polynomials can help identify and separate – at the structural analysis level - the various optical aberrations that may be hidden within the FEA data. As an added benefit, the RMS wavefront error can be estimated directly from the Zernike polynomial coefficients, enabling a quick check of the severity of the various aberrations. Finally, interferometers can report surface deformations as Zernike polynomial coefficients. By transforming FEA results into the same format, correlation between test and analysis is simplified.

However, like all tools, the utilization of Zernike polynomials to represent the finite element deformations of optical surfaces can be misused, misapplied, or misinterpreted. If the FEA deformations have high spatial frequencies (like quilting from a highly lightweighted mirror), a very large number of polynomials would have to be used in order to get a reasonably accurate fit. For some optical components, Zernike polynomials may simply not be appropriate; Wyant and Creath[5] mention that alignment errors of conical optical elements cannot be accurately represented by Zernike polynomials without additional terms. Noncircular apertures and obscurations of all types will lead to errors in the Zernike coefficients, and therefore the representation of the deformed surface. If the optical aberrations are of fairly low order, it can be more efficient and more accurate to compute an integrated optical-structural solution directly in the finite element analysis program. We caution users to inspect both the RMS deviation and the surface shape of the deviations between the FEA data and the fitted Zernike polynomials when using these algorithms. Only then can it be determined if the data translation process is appropriate for the circumstances.

3. GLOBAL VS LOCAL DATA FITTING

It is useful to distinguish two methodologies in the polynomial representation of a data set: global methods and local methods. We classify the use of Zernike polynomials to model surface deformations as a global method of data fitting in that all of the datapoints on the optical surface are fit simultaneously. There are other polynomials that can be used to model surface deformations including XY, Fourier, and Legendre. Local methods of data fitting (i.e., the generation of "hitmaps") involve data interpolation in the immediate vicinity of each datapoint. The values of the datapoints far away do not influence the local determination.

Global data fitting methods have both advantages and disadvantages. An advantage is that large-scale effects like spherical aberration and first order astigmatism are quickly captured and identified at the fitting level. If a local data fitting method were used, the data would need to be ray traced to determine the global aberrations. When using global fitting methods, the fit error can be inspected during the fitting process, and the fitting process terminated if the fit quality is deemed sufficient. In local methods, the entire dataset must be fit before the fit error can be determined. On the other hand, global methods invariably have many more equations (datapoints) than unknowns (Zernike polynomials). Therefore, the fitting process is an error minimization problem that always loses some information. Additionally, if the order of the global fitting polynomials is too low, high spatial frequency aberrations may be lost.

4. ZERNIKE POLYNOMIALS

We use the Zernike polynomials as shown in Malacara and DeVore[6]. As noted by Genberg et al.[7], other normalizations of these polynomials are possible and in use, in which case the polynomial fits would be the same, but the fitting coefficients would be scaled differently. The polynomial series is theoretically unending in that the polynomial definition is unbounded. However, subsets of the infinite series are typically used for surface fitting. Sets composed of 37 and 66 polynomials are usually found in the literature and in implementations in both optical analysis computer programs and interferometers. The 37 polynomial set is called the "Fringe" ordering, and the 66 polynomial set is typically called the "Standard" ordering. It is important to note that there appears to be no agreement on a standard ordering of the polynomials[7], the user is cautioned to verify that the polynomials being fitted are identical to those being used in the optical analysis program.

The Standard set of 66 polynomials includes all the polynomials with radial power of 10 and lower (Zernike polynomials are only defined with even powers on the radial terms). The azimuthal frequency of the sine and cosine parts of these polynomials reaches the value of 5. The Fringe 37 polynomial set includes a 12^{th} order spherical aberration, and does not include 30 of the high radial frequency/high azimuthal frequency polynomials included in

the Standard set. The ordering correspondence in CODE V is shown below with Standard on the first line and Fringe on the second.

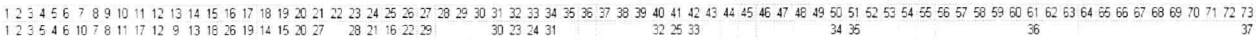

5. ZERNIKE FITTING PROCESS, PART 1

The Zernike fitting process has two major parts: data manipulation, and polynomial fitting. In this section we describe the steps involved with data manipulation and the error sources that should be considered. What we mean by data manipulation is, the effort required to take optical surface deformations predicted by the FEA and to transform them into deformations that are relevant to an optical analysis program. Specifically, the data must be transformed into a topological context different than the typical Cartesian coordinate system used in structural analysis.

Early transformation methods[1,2] appear to have equated the FEA Z displacement with the optical axis Z displacements. This would be accurate for flat optical surfaces, but increasingly in error with increasing radius of curvature. The next generation of algorithms performed the required coordinate transformation from the following point of view: knowing the original location of a gridpoint in a finite element model, and knowing the new location to which the gridpoint has been deformed, what component of this deformation is optically relevant? In this paper, we describe two algorithms that approach the problem from a different point of view: knowing the location where the FEM gridpoint has deformed to, what is the optically relevant deformation back to the original equation of the optical surface.

5.1 Topological Transformations

In the CODE V optical analysis program, optical surface deformations can be described in two different topological contexts: *sag* based and *surface-normal* (wavefront) based. A *sag* based deformation is defined as the distance from the original surface to the deformed surface in a direction parallel to the optical axis of the element. A *surface-normal* based deformation is defined as the distance from the original surface to the deformed surface in a direction perpendicular to the original surface. Both of these are components of the actual node deformation. The surface-normal topological context is also referred to as an interferometer based deformation because interferometers will output surface deformation in this manner. However, the output of a finite element analysis will be in neither of these topological contexts; FEA is performed in Cartesian, cylindrical, or spherical coordinate spaces. Therefore, trigonometric transformations must be performed to change the FEA data into the correct topological context for optical analysis. In the following sections, three algorithms are described to achieve the required transformation in topological context. The first is a sag based transformation with basis in a commercially available computer program[3]. Following it, is a surface-normal transformation and another sag transformation that are the work of the authors.

5.1.1 Algorithm 1

With respect to Figure 1, the distance from P_0 (a gridpoint on the original undeformed surface) to Q (on the deformed surface) is required (call this distance: P_0Q); this is the true sag deformation at the radial and azimuthal location defined by P_0.

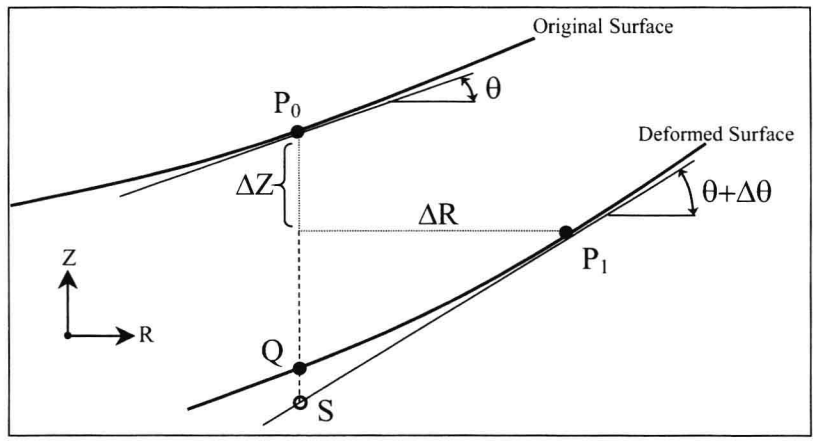

Figure 1. Sag based deformation calculation using only the FEA model and results (Algorithm 1).

However, the gridpoint P_0 has moved to P_1 by virtue of two translations (ΔR and ΔZ) and a rotation about an axis into the page ($\Delta\theta$). The distance P_0Q cannot be exactly calculated because point Q is a phantom location between gridpoints on the finite element model. However, the distance to point S (P_0S) can be calculated and used as an approximation for P_0Q:

$$P_0Q \sim P_0S = \Delta Z - (\Delta R)\tan(\theta + \Delta\theta) \quad (1)$$

Note that θ, which is the slope of the original undeformed surface at P_0, is not reported within the finite element model; this must be computed either by using the three dimensional locations of the immediately surrounding gridpoints, or by using the sag equation of the original surface. Additionally, $\Delta\theta$ will not be computed for finite element models created solely of solid elements; a set of dummy shell elements must be placed on these models so that the in-plane rotational degrees of freedom are retained in the solution set.

5.1.2 Algorithm 2

This algorithm transforms the FEA displacements into the surface-normal, or wavefront topological context. Consider Figure 2; as before, gridpoint P_0 has moved to P_1 by virtue of structural deformations ΔR and ΔZ. However, the location of P_1 is now considered a starting point, and a search is performed to locate the phantom point N on the original optical surface. Point N is defined as the location where the vector normal to the surface passes through the deformed point P_1; the surface-normal deformation is the distance NP_1.

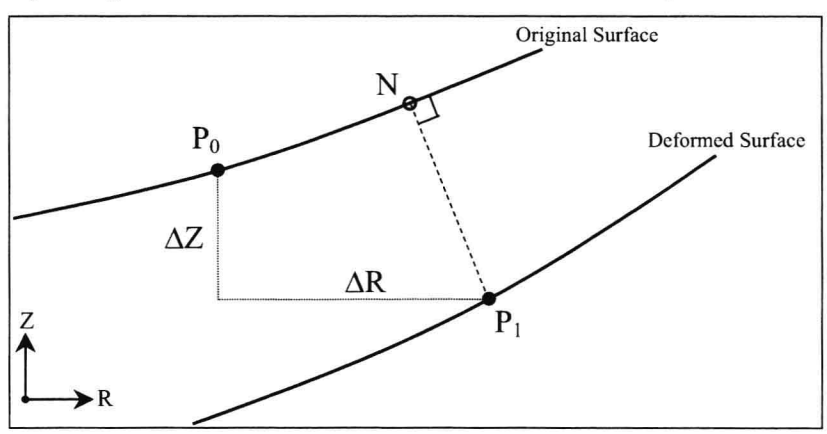

Figure 2. Surface-normal deformation using sag equation of original surface (Algorithm 2).

The surface normal vector is defined as the negative inverse slope of the sag equation at a given point. To accomplish this, a differentiated form of the general aspheric sag equation is used to rapidly compute this vector for the search routine. Note that the surface-normal deformation requires an accurate location for P_1. The deformations (ΔR and ΔZ) are assumed precise, but the original location of P_0 may not be precise due to inaccuracies in the solid modeling of the original surface, in the translation of the surface into the finite element program, in gridpoint generation, and in low precision formatting of the FEA model data. For these reasons, the sag equation of the original surface is used in this algorithm to recompute the precise Z location of P_0 from the listed R,θ coordinates. In this way, the location of P_1 is verified to be accurate.

5.1.3 Algorithm 3

This algorithm transforms the FEA displacements into a sag based topological context. Similar to Algorithm 2, the optically relevant deformation is based on the deformed location, and not the original location. Consider Figure 3 where the original gridpoint P_0 is deformed to P_1 by virtue of radial and axial deformations ΔR and ΔZ. The goal is to compute the length of the vector TP_1, which is parallel to the optical axis, and thereby qualifies as a sag based deformation.

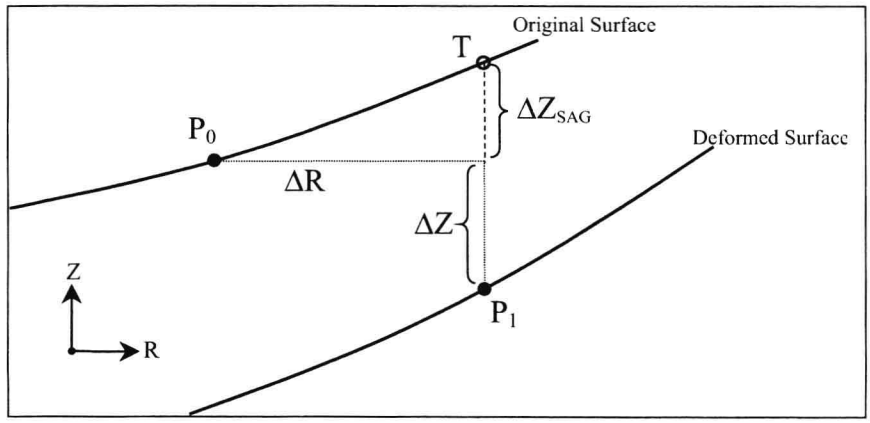

Figure 3. Sag based deformation using sag equation of original surface (Algorithm 3).

The distance TP_1 can be calculated exactly as:

$$TP_1 = \Delta Z + \Delta Z_{sag}, \tag{2}$$

where

$$\Delta Z_{sag} = \text{sag equation}(R_{P0}) - \text{sag equation}(R_{P0}+\Delta R). \tag{3}$$

As in the previous algorithm, knowledge of the sag equation of the original surface is required. However, since the location of P_1 never needs to be calculated, inaccuracies in the location of gridpoint P_0 become much less significant than before. In fact, the Z coordinates of the original and deformed surfaces are not used in the computation. This means that the FEM no longer must have a local coordinate system at each optical surface's vertex, but can be located anywhere along the optical axis with no loss in accuracy. A separate paper[8] being written by the authors describes the implementation of this algorithm as a CODE V macro, and presents test case results verifying its accuracy.

5.1.4 Pros and Cons of the different Algorithms

Each of the algorithms have positive and negative aspects depending on the end use of the data. In our experience, the following pros and cons can be offered:

Algorithm 1: Sag context using only Finite Element model data

Pro: general applicability (no sag equation limitations if original surface slope from FEA); can be coded in matrix form to allow active control analysis.

Con: Accuracy depends on surface curvature, Zernikes cannot be compared to interferometer test output, shell elements required in the finite element model.

Algorithm 2: Surface Normal (wavefront) context using sag equation of original surface

Pro: can be compared directly to interferometer test outputs; can be used to compute RMS wavefront error.

Con: requires a differentiable sag equation; conversion to wavefront topology is iterative and time consuming, wavefront surface deformations are treated approximately for ray tracing in CODE V[8].

Algorithm 3: Sag context using sag equation of original surface

Pro: highest accuracy of the three methods, surface can have arbitrary location along the optical axis.

Con: Zernikes cannot be compared to interferometer test output.

6. ZERNIKE FITTING PROCESS, PART 2

After the FEA results have been transformed into an optically relevant topological context, the data may be fitted by Zernike polynomials. Because the Zernike polynomials are orthogonal, fitting should be straightforward. Unfortunately, there are several reasons why orthogonality has been lost at this juncture, and simply fitting the data may not yield an accurate answer. Situations where orthogonality may be lost include undersampling or nonuniform sampling of the data, and configurations where the unit circle assumption of the Zernike polynomials is violated, i.e. due to obscurations or non-circular apertures, or when the optical surface is annular.

6.1 Sampling Issues

Undersampling the deformed surface has been an obstacle in the past for interferometer based Zernike fitting routines and may still be an issue for FEA if the number of gridpoints on the optical surface is low (< ~200) and/or the deformations are complex. In a test case where the predominant aberrations were low order axisymmetric and tetrafoil, the change in the Zernike coefficients between using 4000 gridpoints and 100 gridpoints was small, as shown in Table I. These results are probably optimistic and a different test case may have yielded significantly larger variation. However, due to automeshing tools and the monumental increase in compute power over the past decade, meshing an optical surface with 1000 to 10000 nodes is no longer an issue, and should prevent significant undersampling effects on the Zernike coefficient computations.

Table I. Undersampling effects on Zernike polynomial fitting.

Zernike Polynomial (Standard ordering)	4000 Gridpoints on optical surface	100 Gridpoints on optical surface
Axisymmetric		
1	5.75	5.75
5	-0.77	-0.78
13	0.18	0.20
25	-0.04	-0.05
Tetrafoil		
11	-0.29	-0.32
23	0.15	0.14

A more insidious error has to do with finite element mesh nonuniformity. If the finite element mesh is highly nonuniform (for instance: a much high density of gridpoints around the periphery as opposed to the center), fitting of Zernike polynomials to the data will be skewed. To counter the nonuniformity of the mesh, the fitting process can be altered to include a scalar for each datapoint proportional to its area of influence on the mesh. This technique, called "area weighting"[7] can yield significant accuracy improvements for distorted finite element meshes.

6.2 Non-circular Aperture Issues

When the aperture is not a complete and perfect circle, orthogonality among the Zernike polynomials is lost. Examples of imperfect apertures include the effects of obscurations – say from a secondary mirror and spider – and variations from a perfect disk - like cutouts on the edges of the optical surface - or an annular surface, or for surfaces that are not even circular. The essential problem is that the Zernike polynomials become coupled (or correlated) which complicates the process of finding the best set of polynomial coefficients that minimizes the fit error to the transformed deformations.

Consider that the goal is to compute a list of coefficients that when applied to the corresponding list of Zernike polynomials and then summed, yields the original transformed deformation at each gridpoint. Classically, for data that is continuous over the unit circle, a matrix inversion of a fully orthogonal set of simultaneous equations would yield the optimum set of coefficients. However, if the polynomials are not orthogonal, the matrix inversion results will not necessarily generate the best fit set of coefficients; Wang and Silva[9] explore this concept extensively.

The magnitude of the problem appears to be case specific. Experimentation by the authors has shown that the loss of orthogonality due to the previously mentioned effects can indeed cause significant loss in the quality of the fit. However, it can be argued that if the fit is sufficiently accurate to describe the deformation, then the goal of the fitting process has been achieved, whether or not the fit is the best possible one. Again we will emphasize that the deviation at the gridpoints between the FEA predicted deformation and the fitted Zernike polynomials should be carefully inspected.

We have considered three methods to eliminate - or at least minimize - this problem: the use of Zernike annular polynomials, Gram-Schmidt orthogonalization of the polynomials over the existing data set, and using an iterative optimization routine to find the best set of polynomial coefficients.

Some of the Zernike polynomials have been re-calculated by Mahajan[10] for purely annular surfaces. Unfortunately, it is not a simple matter to apply surface deformations in this form within CODE V. It may be possible that knowing the coefficients of the annular polynomials, a least squares best fit of the circular polynomials could be computed, however, we have not pursued this avenue of investigation. The use of Gram-Schmidt orthogonalization is much more prevalent in the literature, and a relevant description of the technique is given by Malacara and DeVore[6]. We have not fully investigated the numerical advantages and disadvantages of this technique, consequently we have not yet implemented it.

Finally, we have experimented with using optimization routines to minimize the RMS deviation between the transformed deformations and the Zernike polynomials. Initially, the lowest order polynomials are fit to the data using matrix inversion, and the coefficients optimized to minimize the least squares deviation. Then, a few higher order polynomials are added to the computation and the optimized coefficients from the initial set of polynomials are used as a starting point. The optimization now proceeds on all of the polynomials in the new set, including the initial ones, and the process repeated till the fit is deemed sufficient. Although this is rather a brute force solution, it does have the advantage of significantly improving the Zernike polynomial fit. While we have seen that optimization is a useful method for improving the data fit, we may explore Gram-Schmidt orthogonalization in the future as a more robust solution to the problem.

7. SUMMARY AND CONCLUSIONS

The process of moving optical surface deformations from finite element analyses to optical analysis programs has been considered. Specifically, the process involves mapping Zernike circular polynomials onto the deformations. Since optical analysis programs do not accept deformation data in Cartesian coordinate triplets, the data must be

transformed into either a sag-based or wavefront-based coordinate systems. We show two new methods for this transformation which have improved accuracy over algorithms used in commercially available computer programs. Finally, it is important to realize that the best fit set of Zernike polynomials may not be found simply through a matrix inversion solution. This is due to the unavoidable loss of orthogonality among the Zernike polynomials due to the finite sampling of what will usually be a fraction of the required unit circle aperture. Several potential work-arounds are discussed, but in the end, the user must evaluate the RMS deviation and the surface shape of the deviations between the deformed surface and the Zernike polynomial surface to determine if the data fitting has been successful.

ACKNOWLEDGEMENTS

The mathematical assistance of Robert A. Yetka from the Opto-Mechanical Design Department of Raytheon Missile Systems, is gratefully acknowledged.

REFERENCES

1. Genberg, V. L., "Optical surface evaluation", in *Structural Mechanics of Optical Systems*, L. M. Cohen, ed., *Proc. SPIE* **450**, pp. 81-87, 1983.
2. Bella, D. F., "MSC/NASTRAN pre-processor for performing Zernike polynomial analysis", in *Structural Mechanics of Optical Systems II*, A. E. Hatheway, ed., *Proc. SPIE* **748**, p. 89, 1987.
3. Sigfit, from Sigmadyne, Inc., Rochester, NY.
4. PCFRINGE, from RMR Design Group, Inc., Tucson, AZ.
5. Wyant, J. C., and Creath, K. "Basic Wavefront Aberration Theory for Optical Metrology", in *Applied Optics and Optical Engineering, Vol. XI*, 1992
6. Malacara, D., and DeVore, S. L., "Interferogram Evaluation and Wavefront Fitting", in *Optical Shop Testing, Second Edition*, D. Malacara, ed., John Wiley and Sons, New York, NY, 1992.
7. Genberg, V. L., Michels, G. J., and Doyle, K. B., "Orthogonality of Zernike polynomials", in *Optomechanical Design and Engineering 2002*, A. E. Hatheway, ed., *Proc. SPIE* **4771**, pp. 276-286, 2002.
8. Juergens, R. C., and Coronato, P. A. "Improved method for transfer of FEA results to optical codes", *Proc. SPIE* **5174**, 2003, to be published.
9. Wang, J. Y., and Silva, D. E.; "Wave-front interpretation with Zernike polynomials", *Applied Optics,* **19/9**, pp 1510-1518, 1980.
10. Mahajan, V. N., "Zernike annular polynomials for imaging systems with annular pupils", *J. Opt. Soc. Am.*, **71/1**, pp. 75-85, 1981.

CREDITS

Response of Paraboloidal Surfaces to Linear Thermal Gradients

Rex M. Kremer
Raytheon Missile Systems Co., P.O. Box 11337, Bldg. 840, MS/4, Tucson, AZ 85706

ABSTRACT

This paper presents a theoretical (closed-form) solution for the z-axis surface deformations of a linear, homogeneous, unconstrained and isotropic paraboloidal surface subjected to a 3-dimensional linear thermal temperature gradient and soak temperature change. Previously, an equation for the component of the nodal surface displacement in the z direction has been published. Attaching the z-axis component of the nodal surface displacement to the original surface does not accurately describe the final surface. This work extends the previous analysis and presents a polynomial equation for the corrected surface deformation along the z-axis, as well as, the coefficients for the standard Zernike polynomial describing the corrected surface deformation. Also included is a discussion about z-axis temperature gradients across the paraboloidal surface and how to calculate an equivalent soak temperature change.

Keywords: Temperature gradient, thermal gradient, thermo-elastic analysis

1. INTRODUCTION

It is difficult, if not impossible, to maintain thermal soak conditions on an optical system. Therefore, it is often desirable to calculate the deformation of an optical surface in the presence of thermal gradients. Pearson and Stepp[1] and Pearson[2] have developed equations for the axial surface displacements of a linear, homogeneous, unconstrained and isotropic paraboloidal mirror subjected to a 3-dimensional linear thermal gradient profile. The Pearson and Stepp equations have been summarized by Vukobratovich.[3] Genberg and Michaels[4] have shown that applying the z component of the surface displacement to the original surface does not correctly describe the deformed surface. Therefore, presented here is a polynomial equation that represents the sag height difference between the original and the deformed surface. The equation is generic and can be applied to any paraboloidal surface regardless of the shape of the support structure, e.g. single-arch or double-arch, because the linear thermal gradients applied to a material with a linear coefficient of thermal expansion (CTE) produce displacements but no stresses in the material. A simple method that can be used to relate a linear z-axis gradient to an equivalent soak temperature change is also included.

2. AXIAL COMPONENTS OF THE SURFACE DEFORMATION

Pearson and Stepp developed equations describing displacements due to change in soak temperature (C_0) and linear temperature gradients (C_1, C_2 and C_3) along x-, y- and z-axes, respectively, beginning with the temperature distribution,

$$T(x,y,z,t) = C_0 + C_1(x) + C_2(y) + C_3(z). \tag{1}$$

The origin of the coordinate system is at the base of the mirror, not at the vertex. For an unconstrained body, the axial displacements, (u, v, w), of any point in a homogenous material (CTE=α) due to the above temperature profile are given by

Proceedings of SPIE Vol. 5176 Optomechanics 2003, edited by Alson E. Hatheway
(SPIE, Bellingham, WA, 2003) · 0277-786X/03/$15.00

$$u(x,y,z,t)=\alpha\left[C_0x+\frac{1}{2}C_1\left(x^2-y^2-z^2\right)+C_2xy+C_3xz\right], \tag{2}$$

$$v(x,y,z,t)=\alpha\left[C_0y+C_1xy+\frac{1}{2}C_2\left(y^2-x^2-z^2\right)+C_3yz\right], \text{ and} \tag{3}$$

$$w(x,y,z,t)=\alpha\left[C_0z+C_1xz+C_2zy+\frac{1}{2}C_3\left(z^2-x^2-y^2\right)\right]. \tag{4}$$

The equation for any point on the surface of a paraboloid with thickness z_0 is

$$z(x,y)=z_0+\frac{x^2+y^2}{2R}. \tag{5}$$

To find the z-axis motion of any point, on the mirror simply substitute the equation of the parabola, Equation (5), into the displacement equations, Equations (3)-(5), to get

$$w(x,y,z,t)=\alpha\left[\left(C_0+C_1x+C_2y\right)\left\{z_0+\frac{x^2+y^2}{2R}\right\}+\frac{1}{2}C_3\left(\left\{z_0+\frac{x^2+y^2}{2R}\right\}^2-x^2-y^2\right)\right]. \tag{6}$$

Expanding and rearranging in terms of r ($r^2=x^2+y^2$, $x=r\cos\theta$, $y=r\sin\theta$) yields the equation given by Pearson and Stepp,

$$w(r,z,t)=\frac{\alpha C_3}{8R^2}r^4+\frac{\alpha C_1}{2R}r^3\cos\theta+\frac{\alpha C_2}{2R}r^3\sin\theta+\left(\frac{\alpha C_3z_0}{2R}-\frac{\alpha C_3}{2}+\frac{\alpha C_0}{2R}\right)r^2+ \tag{7}$$
$$\alpha C_1z_0r\cos\theta+\alpha C_2z_0r\sin\theta+\alpha C_0z_0+\frac{\alpha C_3z_0^2}{2}$$

While Equation (7) accurately describes the component of the point displacement in the z-axis direction, it does not describe the surface deformation or figure error. Consider, for example, a mirror where $z_0=C_1=C_2=C_3=0$ and $C_0>0$. The mirror is at a high temperature soak condition. It is known that the radius of curvature gets larger if the CTE is positive. If the vertex does not move, the actual displacement of the original surface to the deformed surface must be in the -z direction. However, Equation (7) shows that the movement of the point on the surface is in the +z direction. Therefore, equations must be developed to determine the corrected z-axis surface deformation.

3. CORRECTED Z-AXIS SURFACE DEFORMATION EQUATION

Consider a point, or node, on the original surface of a parabola, $P_1=(x_1, y_1, z_1)$, that is subjected to the temperature distribution in Equation (1), see Figure 1. After application of the thermal load, the displaced node location is $P_2=(x_2, y_2, z_2)$. Equation (7) describes the z-axis motion of the node, z_2-z_1. However, the corrected z-axis deformation from P_1 is the distance between P_1 and $P_4=(x_1, y_1, z_4)$, i.e. z_4-z_1, while the z-axis deformation from P_3 is the distance between $P_3=(x_2, y_2, z_3)$ and P_2, i.e. z_2-z_3. P_3 is the point on the original surface directly above (or below) the displaced node. For small deformations the difference between z_4-z_1 and z_2-z_3 is negligible, so either can be considered the corrected z-axis surface deformation.

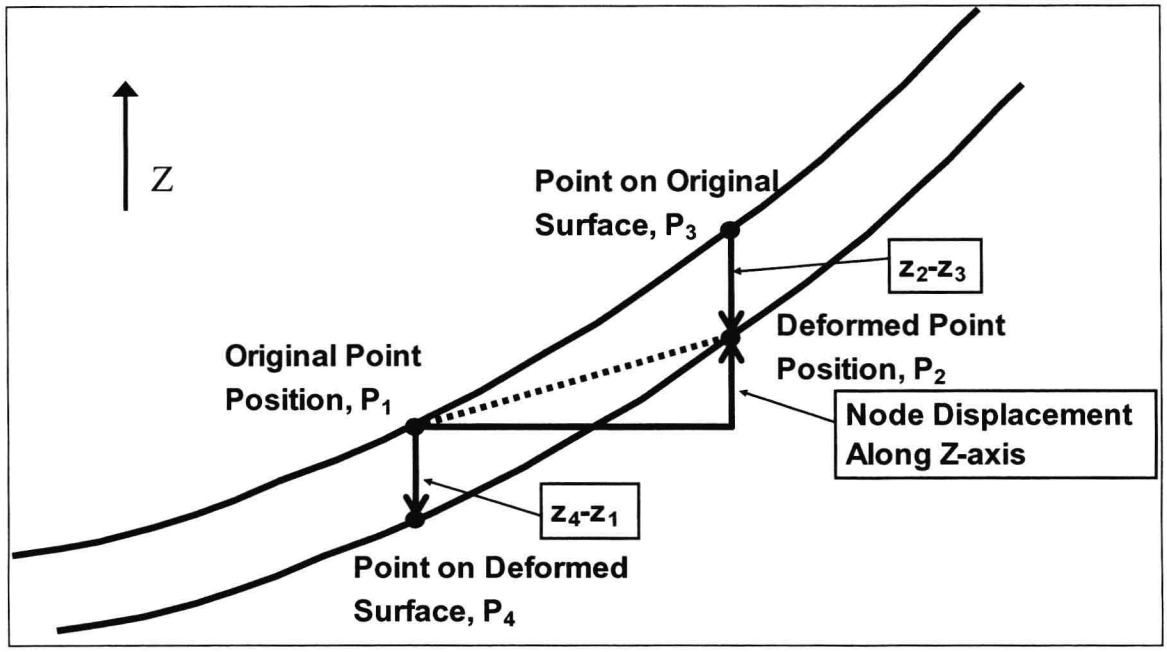

Figure 1: Generic nodal movement due to thermal growth

To calculate the corrected z-axis surface displacement, simply determine the difference between z_2 and z_3 using

$$z_1 = z_0 + \frac{x_1^2 + y_1^2}{2R}, \tag{8}$$

$$z_2 = z_1 + w \quad \text{and} \tag{9}$$

$$z_3 = z_0 + \frac{(x_1+u)^2 + (y_1+v)^2}{2R} = z_1 + \frac{x_1 u + y_1 v}{R} + \frac{u^2+v^2}{2R}. \tag{10}$$

Since u and v contain the (generally) small number α, their squares can be considered negligible compared to the other terms in z_2. The corrected surface deformation is then simply

$$z_2 - z_3 \approx w - \frac{x_1 u + y_1 v}{R}. \tag{11}$$

Collecting on the soak and gradient coefficients (C_0, C_1, C_2 and C_3) yields

$$\begin{aligned} z_2 - z_3 = {} & \alpha C_0 \left[z_1 - \frac{r_1^2}{R} \right] + \alpha C_1 \left[x_1 z_1 - \frac{x_1}{2R}\left(x_1^2 - y_1^2 - z_1^2\right) - \frac{x_1 y_1^2}{R} \right] \\ & + \alpha C_2 \left[y_1 z_1 - \frac{x_1^2 y_1}{R} - \frac{y_1}{2R}\left(y_1^2 - x_1^2 - z_1^2\right) \right] + \alpha C_3 \left[\frac{1}{2}\left(z_1^2 - r_1^2\right) - \frac{r_1^2 z_1}{R} \right] \end{aligned}. \tag{12}$$

Substituting in for z_1 using Equation (5) and reducing leads to the equation of the corrected z-axis surface displacement